Dynamical phase transitions, time-integrated observables, and geometry of states

James M. Hickey, Sam Genway, and Juan P. Garrahan
School of Physics and Astronomy, University of Nottingham, Nottingham, NG7 2RD, United Kingdom
(Received 13 September 2013; published 10 February 2014)

We show that there exist dynamical phase transitions (DPTs), as defined by Heyl *et al*. [Phys. Rev. Lett. **110**, 135704 (2013)], in the transverse-field Ising model (TFIM) away from the static quantum critical points. We study a class of special states associated with singularities in the generating functions of time-integrated observables as found by Hickey *et al*. [Phys. Rev. B **87**, 184303 (2013)]. Studying the dynamics of these special states under the evolution of the TFIM Hamiltonian, we find temporal nonanalyticities in the initial-state return probability associated with dynamical phase transitions. By calculating the Berry phase and Chern number we show the set of special states have interesting geometric features similar to those associated with static quantum critical points.

DOI: 10.1103/PhysRevB.89.054301 PACS number(s): 05.30.Rt, 05.70.Ln

I. INTRODUCTION

Phase transitions are remarkable phenomenon which are ubiquitous in nature and have been studied in equilibrium thermodynamics since the 19th century [1]. Recently, driven by experimental advances [2,3], much interest has turned to the study of nonequilbrium dynamics and phase transitions [2,4–8]. Recent work by Heyl, Polkovnikov, and Kehrein [4] revealed an interesting connection between nonanalyticities in the nonequilibrium dynamics of a quantum system and the theory of equilibrium phase transitions. The authors highlighted the formal similarities between the appearance of nonanalyticities in the return amplitude of a quantum system and the Lee-Yang theory of equilibrium phase transitions [9,10]. Studying in detail the transverse-field Ising model (TFIM), the authors studied quantum quenches across boundaries between the quantum phases as well as quenches within a quantum phase. Only when quenching across a phase boundary were nonanalyticities revealed in the temporal behavior of the return amplitude. In the thermodynamic limit, temporal nonanalyticities emerged due to the coalescence of Lee-Yang zeros in the complex plane of the return amplitude. Due to strong similarities with equilibrium phase transitions they have been dubbed dynamical phase transitions (DPTs) [4].

Other studies, by us and others, have found dynamical insights into many-body dynamics by exploring time-integrated observables [11–13]. Making use of full counting statistics (FCS) methods [12–19], the moment generating function (MGF) for time-integrated observables is treated analogously to a partition sum. In this so-called "s-ensemble" approach, the status of the counting field "s" is elevated to that of a thermodynamic variable [20,21]. Pursuing the thermodynamic analogy, singular features in the long-time behavior of the cumulant generating function (CGF) have been identified as phase transitions in the FCS [22–25]. In a recent paper [26], we studied moments of the time-integrated transverse magnetisation in the TFIM with this formalism and uncovered a set of FCS singularities in the CGF. Analogous to the ground state at the static quantum critical points in the model, there exists a special class of states which capture the singular FCS features. These are eigenstates of the non-Hermitian operator

$$H_s = -\sum_i \sigma_i^z \sigma_{i+1}^z - \left(\lambda + \frac{\mathrm{i}s}{2}\right) \sum_i \sigma_i^x \tag{1}$$

which is related to the MGF. Here, λ is the transverse-field strength and s is the value of the counting field. In Fig. 1 (left) we illustrate the associated set of FCS singularities in the λ-s plane.

In this paper, we explore this special class of states in greater detail. We prepare the system in a right eigenstate of the above non-Hermitian Hamiltonian and study its evolution under the TFIM Hamiltonian ($s = 0$ above) and find DPTs emerge, similar in nature to those uncovered by Heyl, Polkovnikov, and Kehrein in Ref. [4]. Therefore, we demonstrate DPTs can exist *without* performing a quantum quench across a static quantum critical point of the TFIM. In such cases, we find, as in Refs. [4,5,27], nonanalyticities in the initial-state return probability [see Fig. 1 (right)]. We develop further the relation of the special states with ground states near quantum criticality by exploring the geometric properties [28–32] of the class of special states. We find the geometric properties of these states at the FCS singularities exhibit features similar to the ground state at a static quantum critical point [33–35].

The paper is organized as follows: In Sec. II A we provide the theoretical framework on time-integrated observables and FCS criticality in closed systems. We then outline its application to the TFIM in Sec. II B and its connection to the return probability in Sec. III A. In Sec. III B we present our results concerning the connection between these FCS phases and DPTs before providing an overview on the geometric-phase characterization of states and its application to DPTs in Sec. IV A. We then discuss the geometry of the states associated with these FCS phases in Sec. IV B. Finally, we present our conclusions in Sec. V.

II. THEORETICAL FORMALISM

A. Generating functions and time-integrated observables

Central to the theory of phase transitions is the partition function for a system

$$Z(\beta) = \mathrm{Tr}(e^{-\beta H}) = e^{-N\beta f(\beta)} \tag{2}$$

where β is the inverse temperature. Here, $f(\beta)$ is the free energy density, in which nonanalytics associated with phase transitions manifest, and N is the number of degrees of freedom. As noted in Ref. [4], if the system is in a pure state,

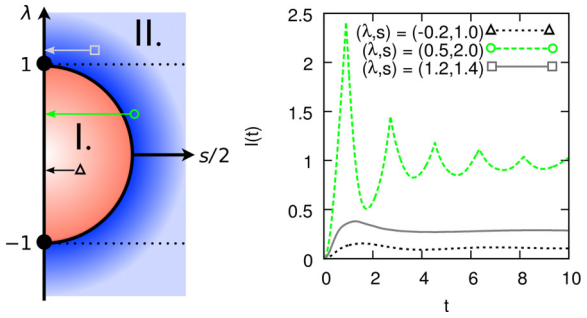

FIG. 1. (Color online) In the left panel is the FCS phase diagram of the TFIM, regions I and II are the dynamically ordered and disordered regimes, respectively [26]. The counting field is labeled s and λ is the transverse magnetic field strength. We consider "quenches" from points $(\lambda,s) \to (\lambda,0)$. The right panel shows the large deviation function associated with the return probability of this protocol. Dynamical nonanalyticities are found when the "quench" crosses the FCS critical line, analogous to the effects of a quantum quench across a static quantum critical point.

the boundary partition function is related to the quantity

$$G(t) = \langle\psi_0|e^{-iHt}|\psi_0\rangle\,. \tag{3}$$

In the context of a quantum quench [2,7] $G(t)$ is the Loschmidt amplitude [36], with H the post-quench Hamiltonian and $|\psi\rangle$ the initial state. Considering now the transfer matrix defined by the Hamiltonian e^{-H}, we define the associated boundary partition function

$$Z(L) = \langle\psi_a|e^{-LH}|\psi_b\rangle, \tag{4}$$

where L is the length of the boundary. Mapping $L \to \beta$ while keeping system size fixed, for $\beta \in \mathbb{C}$, we find if $\beta = it$ and the boundaries are identical ($a = b = 0$) that the analytically continued boundary partition function is the Loschmidt amplitude. In this manner the Loschmidt amplitude relates to the boundary partition function under an analytic continuation in the length of the boundary. This partition function has zeros in the complex β plane which lie on the real time axis (equivalent to imaginary length axis) when $e^{-iHt}|\psi_0\rangle$ is orthogonal to $|\psi_0\rangle$. In the thermodynamic limit these zeros coalesce and may appear as nonanalyticities in the rate function $l(t)$ for the return probability

$$l(t) = \lim_{N\to\infty} \frac{-1}{N} \log|G(t)|^2. \tag{5}$$

It is important to note that, although formally analogous to a boundary partition function, the return probability does not itself provide information on the statistical mechanics of the system. The partition function and Loschmidt amplitude are generating functions for, respectively, the energy of the system (unnormalized) and work done during a quench. These are both static quantities. Singular features in the CGFs (effective free energies) associated with these generating functions correspond to quantum phase transitions and dynamical phase transitions, respectively. We now look at a generating function for purely *dynamical* quantities, namely time-integrated observables [26]. Consider a closed quantum system with a Hamiltonian H. We wish to examine moments of a time-integrated observable

$$Q_t \equiv \int^t q(t')dt', \tag{6}$$

where $q(t')$ is the operator associated with the observable of interest written in the Heisenberg representation. The MGF of this quantity is directly related to a non-Hermitian Hamiltonian H_s and an associated nonunitary evolution operator $T_t(s)$, defined by

$$T_t(s) \equiv e^{-itH_s}, \quad H_s \equiv H - \frac{\mathrm{is}}{2}q\,. \tag{7}$$

With these operators one can show that the MGF of Q_t is given by

$$Z_t(s) = \langle T_t^\dagger(s)T_t(s)\rangle \tag{8}$$

and moments of Q_t are generated through its derivatives, $\langle Q_t^n\rangle = (-)^n\partial_s^n Z_t(s)|_{s\to 0}$, while the logarithm of the MGF, $\Theta_t(s) \equiv \log Z_t(s)$, is the CGF. This forms the definition of a form of FCS [15], where in contrast to the usual definition of FCS we take the parameter s to be real. To study the analytic properties of this generating function it will be useful to study the associated scaled CGF in the long-time limit

$$\theta(s) = \lim_{N,t\to\infty} \frac{\Theta_t(s)}{Nt}. \tag{9}$$

B. Application to the transverse-field Ising model

We focus on the one-dimensional TFIM with periodic boundary conditions, whose Hamiltonian is given by

$$\begin{aligned} H &= -\sum_i \sigma_i^z\sigma_{i+1}^z - \lambda\sum_i \sigma_i^x \\ &= \sum_k \epsilon_k(\lambda)(\gamma_k^\dagger\gamma_k - 1/2)\,, \end{aligned} \tag{10}$$

where $\sigma^{x,z}$ are Pauli matrices and λ is the strength of the magnetic field. The Hamiltonian is diagonalized using a Jordan-Wigner transformation followed by a Bogoliubov transformation [37] and the spectrum (see Appendix) is

$$\epsilon_k(\lambda) = 2\sqrt{(\lambda - \cos k)^2 + \sin^2 k}\,. \tag{11}$$

We examine the generating function associated with the time-integrated transverse magnetization $\sigma^x = \sum_i \sigma_i^x$ when the system is in the ground state. Using standard free-fermion techniques (see Appendix) one finds the CGF [26]

$$\theta(s) = \frac{1}{\pi}\mathrm{Im}\left(\int_0^\pi |\sqrt{(\lambda + is/2 - \cos k)^2 + \sin^2 k}|dk\right). \tag{12}$$

Making an analogy to equilibrium statistical mechanics we treat this CGF as a type of dynamical "free energy" and introduce an order parameter $-\theta'(s)$ and a *dynamical* susceptibility $\chi_s = \theta''(s)$, where $'$ denotes differentiation with respect to s. Using these dynamical quantities the FCS phases can be characterized [see Fig. 1]. A whole critical line exists where χ_s diverges [26]. The static quantum critical points lie at the end of this critical line. This critical curve, shown in Fig. 1, is

a circle in the λ-s plane defined by

$$\lambda^2 + (s/2)^2 = 1. \tag{13}$$

The critical line (13) corresponds to a closing in the gap of the complex spectrum of H_s at a particular wave vector k_λ, which depends on the transverse magnetic field. For $|\lambda| < 1$ the critical s value is given by

$$s_c = 2\sin k_\lambda\,; \quad k_\lambda = \cos^{-1}\lambda\,. \tag{14}$$

This phase diagram is divided into two regions, I and II (see Fig. 1), which we will refer to as *dynamically ordered* and *dynamically disordered*, respectively. Associated with each point in this FCS phase diagram we may associate a state $|s\rangle$ defined by $|s\rangle \equiv \lim_{t\to\infty} T_t(s)|i\rangle$ [26], for initial states $|i\rangle$[1] with an appropriate normalization. The states $|s\rangle$ are right eigenstates of H_s. In our case the initial state is the vacuum of the TFIM. With this choice $|s\rangle$ takes different forms depending on the values of λ and s:

$$|s\rangle = \bigotimes_{k>0} |s_k\rangle$$
$$\propto \begin{cases} \bigotimes_{k>0} |1_k,1_{-k}\rangle_s & \lambda > 1 \\ \bigotimes_{k<k_\lambda} |0_k,0_{-k}\rangle_s \bigotimes_{k>k_\lambda} |1_k,1_{-k}\rangle_s & -1 < \lambda < 1 \\ \bigotimes_{k>0} |0_k,0_{-k}\rangle_s & \lambda < -1 \end{cases} \tag{15}$$

The states $|n_k,n_{-k}\rangle_s$ are eigenstates of H_s with n_k (n_{-k}) fermions in the mode k ($-k$). It turns out that the states $|s\rangle$ can be prepared to high precision by coupling the system to a simple Markovian environment [26]. (Details can be found in the Appendix.) We will study not only the return probability of these states under a "quench" but also their geometric properties.

III. RETURN PROBABILITY AND FCS PHASES

A. Quenches in s

In this paper, we will consider the following quench protocol: We initially connect the Ising chain to an appropriate bath (as in Ref. [26]) and allow it to evolve towards the state $|s\rangle$. After this we will perform a "quench" in the s parameter by decoupling the system from the environment and evolving the state $|s\rangle$ under the TFIM Hamiltonian H:

$$|s_t\rangle = e^{-iHt}|s\rangle = \bigotimes_{k>0} e^{-iHt}|s_k\rangle = \bigotimes_{k>0} |s_{k,t}\rangle. \tag{16}$$

In this scheme, which we will refer to as the "s quench," we will examine how dynamical phase transitions are related to the critical FCS line shown in Fig. 1. Furthermore we will characterize the geometric properties of the states $|s\rangle$ ($|s_t\rangle$), expressed in terms of the Majorana fermions of H, focusing on the Berry phase (Chern number). This approach has previously been used to characterize ground state properties, quantum phase transitions, and DPTs; here, we will use it to characterize the new FCS critical line using states $|s\rangle$. In Sec. IV A we provide a brief discussion of these geometric parameters so we may link these to both quantum as well as FCS phase transitions and connect these critical features with DPTs.

B. The s quench in the TFIM

Having introduced the necessary background to DPTs and the extended set of $|s\rangle$ states we are interested in, we now examine the features of $|s\rangle$ states under the evolution of the TFIM Hamiltonian. From Eqs. (10) and (15) we find that the rate function associated with the return probability [Eq. (5)] takes the form

$$l(t) = -2\mathrm{Re}\left(\int_0^{k_\lambda} \log\left[\frac{|\cos\alpha_k^s|^2 + |\sin\alpha_k^s|^2 e^{-2i\epsilon_k t}}{\cosh 2\mathrm{Im}(\alpha_k^s)}\right] dk + \int_{k_\lambda}^{\pi} \log\left[\frac{|\sin\alpha_k^s|^2 + |\cos\alpha_k^s|^2 e^{-2i\epsilon_k t}}{\cosh 2\mathrm{Im}(\alpha_k^s)}\right] dk\right) \tag{17}$$

with k_λ defined in Eq. (14). In the finite-N regime this function will contain two families of zeros at times

$$t_j^{(1)} = \frac{i}{\epsilon_k}\left(\log|\tan\alpha_k^s|^2 + i(2j+1)\pi\right),$$
$$t_j^{(2)} = \frac{i}{2\epsilon_k}\left(\log|\tan\alpha_k^s|^2 + i(2j+1)\pi\right), \tag{18}$$

for $j \in \mathbb{Z}$. One family of zeros is due to the integrand in Eq. (17) vanishing; the other is attributed to the integrands attaining the same value and emergent nonanalytic behavior at the k_λ limits of these integrals. In both cases these zeros lie on the realtime axis whenever the complex angle α_k^s (see Appendix), is such that $|\cos\alpha_k^s| = |\sin\alpha_k^s|$. This is only ever the case when the initial $|s\rangle$ lies in the dynamically disordered phase and $|\lambda| < 1$ (see Fig. 1): In this region there is a well defined k_λ and the "quench" crosses the FCS critical line described by Eq. (13). Within this regime, in the thermodynamic limit, we see the emergence of nonanalyticities at critical times

$$t_j^* = \frac{(2j+1)\pi}{2\epsilon_{k_\lambda}}, \frac{(2j+1)\pi}{\epsilon_{k_\lambda}}\,. \tag{19}$$

When we prepare the system in a state $|s\rangle$ from within the dynamically ordered regime such that we don't "quench" across the critical line (see Fig. 1), or at $|\lambda| > 1$ where there is no critical line, no DPTs are visible; in this region there is no energy scale k_λ. The interpretation of this energy scale set by k_λ is simple: the occupation of this mode $n_{s=0}(k_\lambda) = 1/2$. The other modes have occupation $n_{s=0}(k) < 1/2$ for $k < k_\lambda$ and $n(k) = 1/2$ for $k > k_\lambda$, so we see k_λ marks the onset of half-occupancy. These results are similar to those in Ref. [4] for ground states with one crucial difference. The emergence of these DPTs is not due to quenching across the static quantum critical point of the model of interest [4–6], the existence of the infinite temperature critical mode was built into the states $|s\rangle$, see Eq. (15). This mode defines the critical features in the FCS of the time-integrated magnetization of this system, and so by creating states which capture such singularities we build in a critical mode k_λ.

To summarize our results in this subsection, we have shown for a particular choice of initial state which is not a ground state of the TFIM, DPT features emerge even far from

[1]This state is independent of the initial state provided the initial state has finite overlap with it.

quantum criticality. We propose that one could even consider the FCS critical line as a critical line for this extended set of states. To corroborate this idea, we will examine the geometric properties of these states in Sec. IV B. Prior to this however it is necessary to introduce the relevant quantities required to study the geometry of these states.

IV. GEOMETRY OF STATES AND DYNAMICAL PHASE TRANSITIONS

A. Geometric phase and Berry curvature

Topological quantum numbers provide an alternative way of classifying and characterizing the ground state properties of many-body quantum systems [34]. This geometric approach to studying ground state properties of many-body systems has provided a new interpretation of quantum phase transitions [38–40]. One of the most widely-used measures of these geometric properties of physical systems is the Berry phase [28] associated with adiabatic transport of quantum state vectors around a closed parameter manifold. Associated with this phase we may construct an associated Berry curvature, which when we consider transport along a two-dimensional manifold M^2 leads to the Chern number of the system. We will now discuss these quantities in more detail, before describing their relationship to results on dynamical quantum phase transitions.

Consider a manifold of Hamiltonians defined by some parameters $\vec{\lambda}$. A natural measure of the distance [41] between the ground states $|0(\vec{\lambda})\rangle$ of this manifold is

$$1-|\langle 0(\vec{\lambda})|0(\vec{\lambda}+d\vec{\lambda})\rangle|^2=\sum_{\mu,\nu}g_{\mu\nu}d\lambda^\mu d\lambda^\nu, \tag{20}$$

where $g_{\mu\nu}$ is the geometric tensor

$$g_{\mu\nu}=\langle 0(\vec{\lambda})|\overleftarrow{\partial_\mu}\partial_\nu|0(\vec{\lambda})\rangle-\langle 0(\vec{\lambda})|\overleftarrow{\partial_\mu}|0(\vec{\lambda})\rangle\langle 0(\vec{\lambda})|\partial_\nu|0(\vec{\lambda})\rangle. \tag{21}$$

Here $\partial_\mu=\partial/\partial\lambda^\mu$ and the diacritic arrow $\leftarrow$ indicates the partial derivative acts to the left. Now the imaginary part of the geometric tensor is directly related to the Berry curvature $F_{\mu\nu}$ via

$$F_{\mu\nu}=-2\mathrm{Im}[g_{\mu\nu}]=\partial_\mu A_\nu-\partial_\nu A_\mu, \tag{22}$$

with $A_\mu=i\langle 0(\vec{\lambda})|\partial_\mu|0(\vec{\lambda})\rangle$ the Berry connection. The line integral of this connection is simply the Berry phase (B) and the surface integral, over the parameter manifold ($\mathcal{M}$), of the curvature is related to a quantity known as the Chern number C:

$$\begin{aligned}B&\equiv\int_{\partial S}\vec{A}.d\vec{\lambda}\\ C&\equiv\frac{1}{2\pi}\int_{\mathcal{M}}F_{\mu\nu}dS_{\mu\nu}.\end{aligned} \tag{23}$$

If the manifold is closed in the topological sense, then the Chern number is simply an integer [42]. We now summarize existing results on two-parameter manifolds which are of relevance to the TFIM [43]. Consider the evolution of the ground state of the TFIM at $\lambda=\lambda_i$ after a quench to λ_f. The time evolved state factorizes into contributions from each momentum sector $|u_{k,t}\rangle$,

$$|u_{k,t}\rangle=[\cos\tilde{\phi}_k-i\sin\tilde{\phi}_k e^{-2i\epsilon_k(\lambda_f)t}\gamma_k^\dagger\gamma_{-k}^\dagger]|0_k,0_{-k}\rangle. \tag{24}$$

The annihilation operators γ_k diagonalize the TFIM Hamiltonian [see Eq. (10)], with ϵ_k (11) the excitation spectrum. The angles $\tilde{\phi}_k$ are the difference between the Bogoliubov angles, associated with the Bogoliubov transformation employed in diagonalizing H, at the initial and final values of λ [37]. The state $|0_k,0_{-k}\rangle$ is the vacuum associated with the mode k ($\gamma_{\pm k}|0_k,0_{-k}\rangle=0$). Examining Eq. (10), one can see that the final Hamiltonian obeys a global $U(1)$ symmetry

$$\gamma_k\to\gamma_k e^{-i\varphi}, \tag{25}$$

however this symmetry is not shared by the time evolved state due to the spontaneous creation of excitations [43]. Furthermore this geometric phase corresponds to the global phase accumulated on cyclic evolution from $\varphi=0$ to π.

We now focus on the manifold of states M^2 defined by parameters k and φ. It is important to note that although we are studying a manifold of quenched states which have an explicit dependence on t, the parameters defining the manifold are time *independent* and hence both the Berry curvature and phase are also time independent. The parameters k and φ are defined on the same interval $[0,\pi]$; this can be seen from the from the form of $|u_{k,t}(\varphi)\rangle$. These states are defined uniquely for $k>0$ and $k<\pi$. Furthermore as the excitations are Cooper-pair-like in nature [see Eq. (24)] the phase factor φ has a factor of 2 preceding it. This implies the states are uniquely defined with $\varphi\in[0,\pi]$. Now in order to compute the curvature of $M^2=[0,\pi]\times[0,\pi]$, we have to compute the derivative of $|u_{k,t}(\varphi)\rangle$ with respect to both φ and k. The derivative with respect to φ is straightforward, while the derivative with respect to k is less so. In order to compute this we need to use perturbation theory and expand $|0_k,0_{-k}\rangle$ as follows:

$$|0_{k+\delta k},0_{-(k+\delta k)}\rangle=|0_k,0_{-k}\rangle+\frac{d}{dk}|0_k,0_{-k}\rangle\delta k+\mathcal{O}(\delta k^2). \tag{26}$$

Standard perturbation theory has an implicit gauge choice built in known as the parallel transport gauge: because the excited states are orthogonal to the ground state, it turns out [44]

$$\frac{d}{dk}|0_k,0_{-k}\rangle=\frac{d}{dk}\gamma_k^\dagger|0_k,0_{-k}\rangle=0, \tag{27}$$

making the calculation of the Berry Phase and curvature straightforward. This manifold was examined with these quenched states in Ref. [43] where it was found that the states $|u_{k,t}(\varphi)\rangle$, at $k=\pi$, are independent of the phase φ,

$$\begin{aligned}&\sin\tilde{\phi}_{k=\pi}=0,\\ &|u_{\pi,t}(\varphi)\rangle=|u_\pi\rangle=\cos\tilde{\phi}_{k=\pi}|0_\pi,0_{-\pi}\rangle.\end{aligned} \tag{28}$$

This behavior is independent of the quench protocol. However, the behavior of the infrared states ($k\to0$) is slightly more complex. If we quench within the same phase the $k=0$ states are φ independent, as $\sin\tilde{\phi}_{k\to0}=0$, and so the manifold M^2 is topologically equivalent to the 2-sphere. However, quenching across the static quantum critical point, we find the $k=0$ states now depend on φ up to a global phase, as

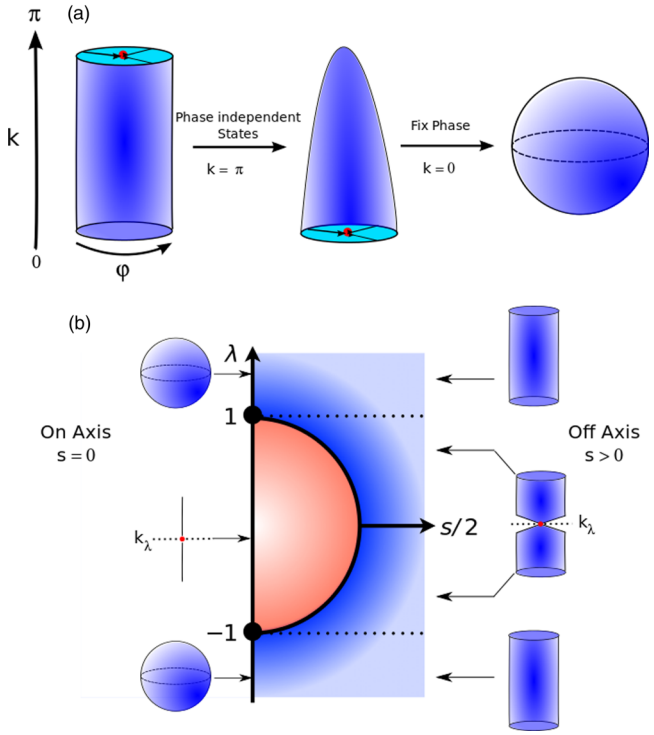

FIG. 2. (Color online) (a) The parameter manifold M^2 is topologically equivalent to the S^2 sphere as the $k = \pi$ mode is φ independent and the $k = 0$ mode is (at most) only dependent on φ up to a gauge transformation. (b) Examining the manifold at each point in the FCS phase diagram we find that at k_λ the manifold is φ independent. The s states below $|\lambda| = 1$ are found to be completely φ independent on the $s = 0$ line. However above the $|\lambda| = 1$ line the manifold once again becomes topologically equivalent to the S^2 sphere at $s = 0$.

$\sin\phi_{k\to 0} = 1$,

$$|u_{0,t}(\varphi)\rangle = -ie^{2i\varphi}e^{-2i\epsilon_k(\lambda_f)t}|1_{k=0}, 1_{k=0}\rangle. \tag{29}$$

This global phase may be removed with an appropriate gauge transformation, once again leading to topological equivalence with a 2-sphere (see Fig. 2). This dependence on φ up to a total phase is due to a population inversion [4] of the modes associated with the quench Hamiltonian on crossing the critical point.

On quenching across the critical point DPTs have been shown to emerge [4]. The appearance of these DPTs is correlated with the need to gauge fix the $k = 0$ modes when examining the topology of our M^2 manifold. This gauge fixing alters the Chern number associated with this manifold of quenched states. In Ref. [43] the Chern number for this manifold was determined to be $C = \sin^2\tilde{\phi}_{k=0}$. For quenches within the same phase $C = 0$, but for quenches across the critical point it was found that $C = 1$. For this system and manifold of states the change in topological number corresponds to the emergence of dynamical phase transitions [43] on quenching across the quantum critical point.

In the next section we apply this idea of geometric phase using the set of states $|s_{k,t}\rangle$, defined in Eqs. (15) and (16), in place of the $|u_{k,t}\rangle$ states. By studying the dynamical properties of our s quench and the geometric properties of the s states we will extend the links between the geometric phase and both static and dynamical criticality to the FCS critical line in the TFIM.

B. Geometry of s states

Now we turn to a geometric characterization of the states $|s\rangle$ (15) and $|s_t\rangle$ (16), beginning with an analysis of the former. These states, $|s\rangle$, are the right eigenvectors of H_s. Previously it has been shown [34,38–40] that the geometry of a system's ground state shows signatures of static quantum critical points. By analogy we expect that the geometric properties of these states, $|s\rangle$, should show signatures of the FCS critical line (13). However, as this is not a conventional quantum critical line it is unclear exactly how these geometric quantities such as the Berry phase and Chern number will behave in its vicinity. We begin by introducing a family of TFIM Hamiltonians $H(\varphi)$ which depend on the parameter φ associated with the global phase shift of fermionic operators (25). Diagonalizing both H_s and H we are able to express the FCS-critical state $|s\rangle$ in terms of the fermionic modes of the final Hamiltonian H. Applying a global phase shift $\gamma_k \to \gamma_k e^{-i\varphi}$, as in Sec. IV A, to the fermionic operators of H, we obtain a state $|s(\varphi)\rangle$, see Appendix. From Eq. (23), the Berry phase associated with this adiabatic evolution is given by

$$B = \int_0^\pi \langle s(\varphi)|i\partial_\varphi|s(\varphi)\rangle d\varphi. \tag{30}$$

To study the FCS critical line it is necessary to work in the thermodynamic limit where the size of the spin chain $N \to \infty$. In this limit we study the geometric density, $\tilde{\beta} \equiv \lim_{N\to\infty} B/N$, and inserting $|s(\varphi)\rangle$ in Eq. (30) we find it takes the form

$$\tilde{\beta} = -\int_{k_\lambda}^{\pi} \frac{|\cos\alpha_k^s|^2}{\cosh 2\mathrm{Im}(\alpha_k^s)}dk - \int_0^{k_\lambda} \frac{|\sin\alpha_k^s|^2}{\cosh 2\mathrm{Im}(\alpha_k^s)}dk. \tag{31}$$

In Fig. 3 we plot $\tilde{\beta}$ for some representative slices through the (λ, s) plane. The geometric phase density appears to be the same in both regions I and II of the FCS phase diagram, see Figs. 1 and 3. However on examining $d\tilde{\beta}/ds$, minima appear at the FCS critical line. Previously such extrema were used as a method to identify quantum criticality [33,38–40], but here they also mark the critical features not of the final Hamiltonian but of H_s.

We have shown that the Berry phase can be used as a method to identify FCS critical points. We note that this is due to the connection of the Berry phase and the energy-level structure of H_s. To connect this observation with the emergence of DPTs we perform an analysis of the Chern number C discussed in Sec. IV A. Still working in the thermodynamic limit we now consider the "quenched" state $|s_t(\varphi)\rangle$, with φ still denoting the fermionic shift defined in Eq. (25), and split it up into its contributions from each momentum sector k. Combining the result with Eq. (23), the Chern number has a highly nontrivial functional form

$$C = \frac{2\left(|\cos\alpha_{k_\lambda}^s|^2 - |\sin\alpha_{k_\lambda}^s|^2\right)}{\cosh 2\mathrm{Im}(\alpha_{k_\lambda}^s)} + \mathrm{Im}\left(\int_0^{k_\lambda} \frac{2i\left(\sin\alpha_k^s\right)^* \cos\alpha_k^s \partial_k \alpha_k^s}{\cosh 2\mathrm{Im}(\alpha_k^s)}dk\right)$$

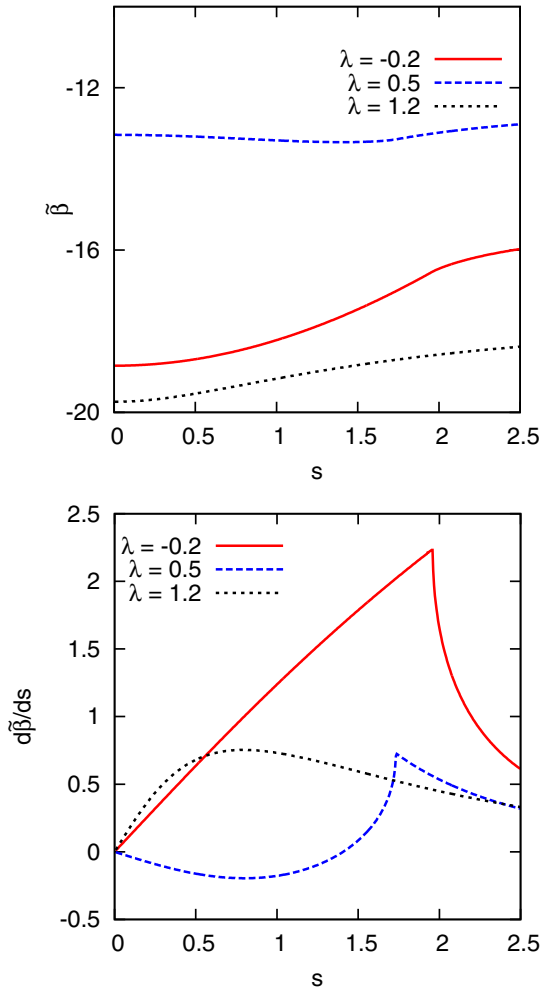

FIG. 3. (Color online) The top panel shows slices of the Berry phase density at various λ values. No extremum or singular features are visible in the vicinity of the FCS critical line, see Fig. 1. However, the derivative of this density $d\tilde{\beta}/ds$ has extremum located at the FCS critical line; this is shown in the bottom panel. For $|\lambda| > 1$ no such extremum are present; this is due to a lack of any FCS critical points in this parameter regime.

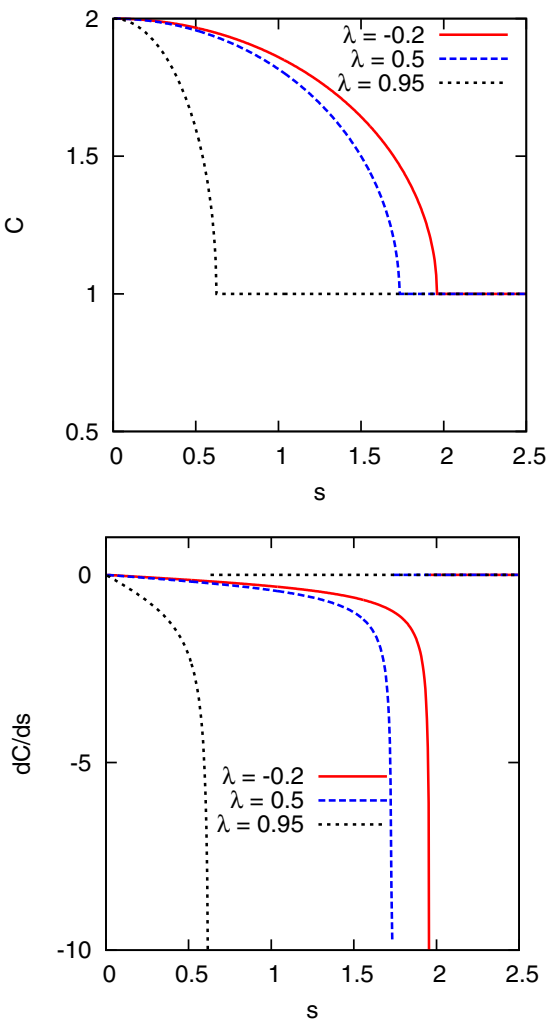

FIG. 4. (Color online) The Chern number C associated with the manifold of $|s_{k,t}\rangle$ states has a "kink" at the FCS critical line; this is shown for various λ slices in the top panel. The derivative of the Chern number displays divergences at the FCS critical line; these features are usually associated with quantum criticality but now mark the FCS critical line, bottom panel.

$$
\begin{aligned}
&-\mathrm{Im}\left(\int_{k_\lambda}^{\pi} \frac{2i\left(\cos\alpha_k^s\right)^* \sin\alpha_k^s \partial_k \alpha_k^s}{\cosh 2\mathrm{Im}\left(\alpha_k^s\right)} dk\right)\\
&-\mathrm{Im}\left(\int_{k_\lambda}^{\pi} \frac{2i\left|\cos\alpha_k^s\right|^2\left(\cos\alpha_k^s\left(\sin\alpha_k^s\right)^* - \mathrm{H.c.}\right)\partial_k \alpha_k^s}{\cosh^2 2\mathrm{Im}\left(\alpha_{k_\lambda}^s\right)} dk\right)\\
&-\mathrm{Im}\left(\int_{0}^{k_\lambda} \frac{2i\left|\sin\alpha_k^s\right|^2\left(\cos\alpha_k^s\left(\sin\alpha_k^s\right)^* - \mathrm{H.c.}\right)\partial_k \alpha_k^s}{\cosh^2 2\mathrm{Im}\left(\alpha_{k_\lambda}^s\right)} dk\right).
\end{aligned}
\tag{32}
$$

Here the superscript $*$ denotes complex conjugation and H.c. denotes the Hermitian conjugate. We plot C as a function of s for different values of λ in Fig. 4. We recall that in Sec. IV A using the ground state for the case of the TFIM [43] it was shown when quenching within a phase led to a Chern number of 0, while quenching across the critical point led to a change in topological quantization and $C = 1$. That these values are integers is attributed to the fact that the ground-state parameter manifold is topologically equivalent to a S^2 sphere, as discussed in Sec. IV A. For the states we have studied, for $s \neq 0$ the manifold of the states $|s_{k,t}(\varphi)\rangle$ does not possess the same properties as that of $|u_{k,t}(\varphi)\rangle$. These states depend nontrivially on $\varphi \forall (k \neq k_\lambda)$, and so M^2 is cylindrical in nature. Below $|\lambda| = 1$, the state defined by k_λ does not depend on φ and so the cylinder is "pinched" at this point. We illustrate these topologies in Fig. 2. These manifolds all possess boundaries and so display noninteger Chern numbers, however on taking the limit of $s \to 0$ the manifolds become much simpler. Above $|\lambda| = 1$ they once again become equivalent to a S^2 sphere, and in the statically ordered phase $|\lambda| < 1$, all φ dependence is lost.

The Chern number C has a nonanalytic point precisely at the FCS critical line, see Fig. 4. This "kink" is similar to that observed in the dynamical order parameter $-\theta'(s)$ discussed in Sec. II B and in Ref. [26]. Examining the derivative dC/ds,

we see it diverges at the critical line in a manner very similar to χ_s. We note that the FCS critical line is associated with a closing of the gap of an *excited state* in the complex spectrum of H_s [26]. One may expect that the closing of such a gap would lead to divergences in the Berry phase and not extrema. The emergence of extrema is due to our choice of initial state: While the gap in H_s is single particle in nature, the multiparticle states $|s\rangle$ ($|s_t\rangle$) are of a construction such that in the thermodynamic limit the single-particle divergences are suppressed and we see extrema. These features indicate that the FCS critical line of the TFIM can be thought of as a static quantum critical line of some other Hermitian Hamiltonian. However, in contrast to the non-Hermitian H_s, it is not easy to see how to construct such a Hamiltonian in a way that is directly related to that of the TFIM.

V. CONCLUSIONS

In this paper we examined singularities of the generating function of time-integrated observables from the perspective of DPTs, as defined in Ref. [4], and geometric phase. We focused on the example of the TFIM and the time-integrated transverse magnetization. Previously it was shown that using suitable external environments one may prepare the system in specific states $|s\rangle$, which capture this FCS criticality. We demonstrated, using such states, that even *far from quantum criticality* of the TFIM one may observe DPTs and that these DPTs only emerge when one "quenches" across the FCS critical line. A recent work [27] highlighted a similar observation in the XXZ chain, where DPTs emerged when quenching within the gapped phase. This was attributed to the steady state behavior of the system. In contrast in this paper we find that the emergence of DPTs is not due to the steady state behavior but to our *initial state*. We then characterized this FCS critical line by studying the geometry of these states. We found that the derivative of the Berry phase with respect to the s parameter exhibited an extremum at the FCS critical line. Similarly the derivative of the Chern number diverged at this phase boundary. These results are similar to previous approaches to identifying static quantum critical points using the geometric phase. This link between FCS criticality and the geometry of these s states requires further investigation along with the examination of time-integrated observables in other models to see if this connection still holds. Furthermore a direct link between the generating functions of time-integrated observables and geometric quantities would be interesting and will be a focus of future work.

ACKNOWLEDGMENTS

We thank A. Polkovnikov for useful comments on the manuscript. This work was supported by EPSRC Grant No. EP/I017828/1 and Leverhulme Trust Grant No. F/00114/BG.

APPENDIX A: DIAGONALIZATION OF H_s/H AND THE s STATE

To study the time-integrated magnetization of the TFIM we must diagonalize the non-Hermitian Hamiltonian H_s; this can be done via a Jordan-Wigner transformation in combination with a Bogoliubov rotation [37]. Then taking the $s \to 0$ limit one also obtains the diagonalized form of the original Hamiltonian H.

The Jordan-Wigner transformation expresses the Pauli spin operators σ_i^x, σ_i^+, and σ_i^- at site i in terms of corresponding fermionic operators c_i and $c_i^\dagger$ with $\{c_i^\dagger, c_j\} = \delta_{i,j}$ as

$$\begin{aligned}\sigma_i^x &= 1 - 2c_i^\dagger c_i,\\ \sigma_i^+ &= \prod_{j<i}(1-2c_j^\dagger c_j)c_i,\\ \sigma_i^- &= \prod_{j<i}(1-2c_j^\dagger c_j)c_i^\dagger.\end{aligned} \tag{A1}$$

This Hamiltonian is translationally invariant and so we change to the Fourier representation

$$c_i = \frac{1}{\sqrt{N}}\sum_k e^{-ikr_i}c_k \tag{A2}$$

and rewrite the Hamiltonian as

$$\begin{aligned}H_s = &-\sum_k (2(\cos k - (is/2+\lambda)))c_k^\dagger c_k\\ &- i\sin k(c_{-k}c_k + c_{-k}^\dagger c_k^\dagger).\end{aligned} \tag{A3}$$

For specificity we restrict ourselves to an even number of spins N, and with periodic boundary conditions, the discrete wave vector k takes values $k = \pi n/N$ where $n = -N+1, -N+3, \ldots, N-1$.

We note that the Hamiltonian in Eq. (A3) contains terms that do not conserve the number of fermions, for instance $c_{-k}^\dagger c_k^\dagger$. These terms are eliminated next via a canonical Bogoliubov rotation. This transformation expresses the Jordan-Wigner operators as a linear combination of a set of s-dependent fermionic operators c_k and $c_k^\dagger$ with $\{c_k, c_{k'}^\dagger\} = \delta_{k,k'}$ as

$$\begin{aligned}c_k &= \cos\frac{\phi_k^s}{2}A_k + i\sin\frac{\phi_k^s}{2}\bar{A}_{-k},\\ c_k^\dagger &= \cos\frac{\phi_k^s}{2}\bar{A}_k - i\sin\frac{\phi_k^s}{2}A_{-k}.\end{aligned} \tag{A4}$$

Here we have a complex fermionic pair, $\{\bar{A}_{k'}, A_k\} = \delta_{k',k}$, where $\bar{A}_k \neq A_k^\dagger$. In the limit $s \to 0$ this fermionic pair reduces to a more canonical form, $\bar{A}_k \to \gamma_k^\dagger$ and $A_k \to \gamma_k$. These complex Bogoliubov angles ϕ_k^s satisfy

$$\phi_{-k}^s = -\phi_k^s \tag{A5}$$

and are chosen such that only terms that conserve the number of fermions are present in the Hamiltonian; note in the limit of $s \to 0$, this angle becomes $\phi_k^{s=0} = \phi_k$. To enforce this condition, the Bogoliubov angles must satisfy

$$\tan\phi_k^s = \frac{\sin k}{is/2 + \lambda - \cos k}. \tag{A6}$$

With this choice we arrive at the free-fermion dispersion relation given:

$$\epsilon_k(\lambda, s) = 2\sqrt{(\lambda + is/2 - \cos k)^2 + \sin^2 k}. \tag{A7}$$

Now the key property for expressing the fermionic states of the $s = 0$ Hamiltonian in terms of the fermionic states of H_s

is to notice that the ground state of H may be expressed as a BCS state of H_s:

$$|0\rangle = \frac{1}{\mathcal{N}'}\exp\left(\sum_{k>0} B(k)\bar{A}_k\bar{A}_{-k}\right)|0\rangle_s \propto \bigotimes_{k>0}\left[\cos\alpha_k^s|0_k,0_{-k}\rangle_s - i\sin\alpha_k^s|1_k,1_{-k}\rangle_s\right]. \quad \text{(A8)}$$

In this equation (A8) $|0_k,0_{-k}\rangle_s$ is the k-mode vacuum, $A_k|0_k,0_{-k}\rangle_s = A_{-k}|0_k,0_{-k}\rangle_s = 0$, and $\bar{A}_k\bar{A}_{-k}|0_k,0_{-k}\rangle_s = |1_k,1_{-k}\rangle_s$ indicate occupation states of the fermionic modes with $|k|$ that diagonalize H_s. The complex angles appearing in the coefficients are directly related to the Bogoliubov angles by $\alpha_k^s = \frac{\phi_k-\phi_k^s}{2}$. This BCS form may be easily inverted and the fermionic occupation states, appropriately normalized, of H_s are related to their $s=0$ counterparts via

$$|0_k,0_{-k}\rangle_s = \frac{1}{\sqrt{\cosh 2\mathrm{Im}(\alpha_k^s)}}\left(\cos\alpha_k^s|0_k,0_{-k}\rangle - i\sin\alpha_k^s|1_k,1_{-k}\rangle\right),$$
$$|1_k,1_{-k}\rangle_s = \frac{1}{\sqrt{\cosh 2\mathrm{Im}(\alpha_k^s)}}\left(\cos\alpha_k^s|1_k,1_{-k}\rangle - i\sin\alpha_k^s|0_k,0_{-k}\rangle\right). \quad \text{(A9)}$$

We now consider the s-quench protocol described in the main text. We firstly connect the Ising chain, prepared in its ground state, to a bath and allow it to evolve to the s state,

$$|s\rangle = \bigotimes_{k>0}|s_k\rangle,$$
$$|s_k\rangle = \tau(k_\lambda - k)|0_k,0_{-k}\rangle_s + \tau(k-k_\lambda)|1_k,1_{-k}\rangle_s + \delta_{k,k_\lambda}|0_{k_\lambda},0_{-k_\lambda}\rangle. \quad \text{(A10)}$$

here $\tau(x)$ is the Heavi-side step function. After this we will evolve the state using it's original $s=0$, Hamiltonian. Expressing these H_s fermionic states in terms of their original $s=0$ counterparts, this evolution may be evaluated analytically. The time evolved s state may still be expressed as a product of contributions from each momentum sector

$$\begin{aligned}|s_{k,t}\rangle &= \tau(k_\lambda-k)\frac{1}{\mathcal{N}}\left(\cos\alpha_k^s - i\sin\alpha_k^s e^{-2i\epsilon_k t}\gamma_k^\dagger\gamma_{-k}^\dagger\right)|0_k,0_{-k}\rangle \\ &+ \tau(k-k_\lambda)\frac{1}{\mathcal{N}}\left(-i\sin\alpha_k^s + \cos\alpha_k^s e^{-2i\epsilon_k t}\gamma_k^\dagger\gamma_{-k}^\dagger\right)|0_k,0_{-k}\rangle \\ &+ \delta_{k,k_\lambda}\left[\cos\phi_{k_\lambda} - i\sin\phi_{k_\lambda}e^{-2i\epsilon_{k_\lambda}t}\gamma_{k_\lambda}^\dagger\gamma_{-k_\lambda}^\dagger\right]|0_{k_\lambda},0_{-k_\lambda}\rangle. \end{aligned} \quad \text{(A11)}$$

The normalization is related to the imaginary components of α_k^s given by $\mathcal{N} = \sqrt{\cosh 2\mathrm{Im}(\alpha_k^s)}$. By performing a global phase shift, $\gamma_k \to \gamma_k e^{-i\varphi}$, we obtain $|s_{k,t}(\varphi)\rangle$ and $|s(\varphi)\rangle$.

APPENDIX B: DERIVATION OF $\theta(s)$ AND PREPARATION OF $|s\rangle$

Expressing the initial ground state as a BCS state as in Eq. (A8) and evolving it using the nonunitary evolution operator $T_t(s)$, we find the MGF as defined in Eq. (8) takes the form

$$\begin{aligned}Z(s,t) = \prod_{k>0}\Big(&|\cos\alpha_k^s|^2\cosh\left[2\mathrm{Im}(\alpha_k^s)\right]e^{-2\mathrm{Im}(\epsilon_k^s)t} \\ &+ |\sin\alpha_k^s|^2\cosh\left[2\mathrm{Im}(\alpha_k^s)\right]e^{2\mathrm{Im}(\epsilon_k^s)t} \\ &+ i\sin\alpha_k^s\cos\alpha_k^{-s}\sinh\left[2\mathrm{Im}(\alpha_k^s)\right]e^{-2i\mathrm{Re}(\epsilon_k^s)t} \\ &- i\sin\alpha_k^{-s}\cos\alpha_k^s\sinh\left[2\mathrm{Im}(\alpha_k^s)\right]e^{2i\mathrm{Re}(\epsilon_k^s)t}\Big).\end{aligned} \quad \text{(B1)}$$

Now that $\theta(s)$ is the appropriately scaled CGF, see Eq. (9), in the longtime limit the CGF obtains a contribution from each k mode above given by $2|\mathrm{Im}\epsilon_k^s|$. Dividing by N the sum over these k mode contributions becomes an integral, and we find

$$\theta(s) = \lim_{N\to\infty}\frac{2}{N}\sum\left|\mathrm{Im}\epsilon_k^s\right| = \frac{1}{\pi}\mathrm{Im}\left(\int_0^\pi\left|\sqrt{(\lambda+is/2-\cos k)^2+\sin^2 k}\right|dk\right). \quad \text{(B2)}$$

Above we've used the identity $\frac{1}{N}\sum_{k>0}\to\frac{1}{2\pi}\int_0^\pi dk$, which is valid in the thermodynamic limit. From here we will now outline how one may prepare the system in the $|s\rangle$ state using appropriate Markovian baths. The $|s\rangle$ state is the state obtained under evolution from $T_t(s)$; this operator defines the evolution of a density matrix $\rho(t)$ as $\dot{\rho}(t) = -i[\hat{H},\rho(t)] - \frac{s}{2}\{q,\rho(t)\}$. This is the same as a Lindblad master equation, $\dot{\rho} = -i[\hat{H},\rho] + \sum_i(L_i\rho L_i^\dagger - \frac{1}{2}\{L_i^\dagger L_i,\rho\})$, although without the recycling terms. Hence the effective evolution defined by $T_t(s)$ is that of a dissipative Ising chain where no quanta have been emitted into the bath [26,45].

In this problem we are interested in time integrals of the total transverse magnetization, i.e., $q=\sum_i\sigma_i^x$. To construct the simple Markovian environment whose no jump evolution effectively matches that of $T_t(s)$ we apply a trivial shift to q so that $q\to\sum_i(\sigma_i^x+1)$, and now we may identify with a set of quantum jump operators L_i such that $\sum_i L_i^\dagger L_i = s\sum_i(\sigma_i^x+1)$. With such an identification we can choose quantum jump operators $L_i = \sqrt{2s}|-\rangle_i\langle+|_i$; now s plays the role of a decay rate, and $\sigma_i^x|\pm\rangle_i = \pm|\pm\rangle_i$. Now to evolve to the $|s\rangle$ state, we connect the Ising chain to this Markovian environment, and if it evolves without emission for a longtime t then we obtain the $|s\rangle$ state. This procedure was implemented using a cold ion system in Ref. [26].

[1] J. C. Maxwell, Nature (London) **11**, 357 (1875).

[2] A. Polkovnikov, K. Sengupta, A. Silva, and M. Vengalattore, Rev. Mod. Phys. **83**, 863 (2011).

[3] G. Greiner, O. Mandel, T. Esslinger, T. Hänsch, and I. Bloch, Nature (London) **419**, 51 (2002); T. Kinoshita, T. Wenger, and D. Weiss, *ibid.* **440**, 900 (2006); M. Gring, M. Kuhnert, T. Langen, T. Kitagawa, B. Rauer, M. Schreitl, I. Mazets, D. A. Smith, E. Demler, and J. Schmiedmayer, Science **337**, 1318 (2012); M. Cheneau, P. Barmettler, D. Poletti, M. Endres, P. Schauß, T. Fukuhara, C. Gross, I. Bloch, C. Kollath, and S. Kuhr, Nature (London) **481**, 484 (2012).

[4] M. Heyl, A. Polkovnikov, and S. Kehrein, Phys. Rev. Lett. **110**, 135704 (2013).

[5] C. Karrasch and D. Schuricht, Phys. Rev. B **87**, 195104 (2013).

[6] F. Pollmann, S. Mukerjee, A. G. Green, and J. E. Moore, Phys. Rev. E **81**, 020101 (2010).

[7] A. Gambassi and A. Silva, Phys. Rev. Lett. **109**, 250602 (2012).

[8] P. Calabrese, F. H. L. Essler, and M. Fagotti, Phys. Rev. Lett. **106**, 227203 (2011); J. Stat. Mech. (2012) P07016; (2012) P07022; D. Schuricht and F. H. L. Essler, *ibid.* (2012) P04017.

[9] T. D. Lee and C. N. Yang, Phys. Rev. **87**, 410 (1952); C. N. Yang and T. D. Lee, *ibid.* **87**, 404 (1952).

[10] M. E. Fisher in *Lectures in Theoretical Physics*, editted by W. E. Brittin, Vol. 7c (University of Colorado Press, Boulder, 1965).

[11] D. Ruelle, *Thermodynamic formalism* (Cambridge University Press, Cambridge, UK, 2004).

[12] V. Lecomte, C. Appert-Rolland, and F. van Wijland, J. Stat. Phys. **127**, 51 (2007).

[13] J. P. Garrahan, R. L. Jack, V. Lecomte, E. Pitard, K. van Duijvendijk, and F. van Wijland, Phys. Rev. Lett. **98**, 195702 (2007).

[14] L. S. Levitov and G. B. Lesovik, JETP Lett. **58**, 230 (1993); L. S. Levitov, H. Lee, and G. B. Lesovik, J. Math. Phys. **37**, 4845 (1996).

[15] *Quantum Noise in Mesoscopic Physics*, edited by Y. V. Nazarov (Kluwer Academic Publishers, Dordrecht, The Netherlands, 2003); Y. V. Nazarov and M. Kindermann, Eur. Phys. J. B **35**, 413 (2003).

[16] S. Pilgram, A. N. Jordan, E. V. Sukhorukov, and M. Büttiker, Phys. Rev. Lett. **90**, 206801 (2003).

[17] C. Flindt, T. Novotný, A. Braggio, M. Sassetti, and A.-P. Jauho, Phys. Rev. Lett. **100**, 150601 (2008).

[18] M. Esposito, U. Harbola, and S. Mukamel, Rev. Mod. Phys. **81**, 1665 (2009).

[19] C. Flindt, C. Fricke, F. Hohls, T. Novotný, K. Netocny, T. Brandes, and R. J. Haug, Proc. Natl. Acad. Sci. USA **106**, 10116 (2009).

[20] L. O. Hedges, R. L. Jack, J. P. Garrahan, and D. Chandler, Science **323**, 1309 (2009).

[21] E. Pitard, V. Lecomte, and F. van Wijland, Europhys. Lett. **96**, 56002 (2011); T. Speck and D. Chandler, J. Chem. Phys. **136**, 184509 (2012).

[22] C. Ates, B. Olmos, J. P. Garrahan, and I. Lesanovsky, Phys. Rev. A **85**, 043620 (2012).

[23] J. P. Garrahan and I. Lesanovsky, Phys. Rev. Lett. **104**, 160601 (2010).

[24] S. Genway, J. P. Garrahan, I. Lesanovsky, and A. D. Armour, Phys. Rev. E. **85**, 051122 (2012).

[25] J. M. Hickey, S. Genway, I. Lesanovsky, and J. P. Garrahan, Phys. Rev. A **86**, 063824 (2012).

[26] J. M. Hickey, S. Genway, I. Lesanovsky, and J. P. Garrahan, Phys. Rev. B **87**, 184303 (2013).

[27] M. Fagotti, arXiv:1308.0277.

[28] M. V. Berry, Proc. R. Soc. London, Ser. A **392**, 45 (1984).

[29] B. Simon, Phys. Rev. Lett. **51**, 2167 (1983).

[30] Y. Aharonov and J. Anandan, Phys. Rev. Lett. **58**, 1593 (1987).

[31] J. Samuel and R. Bhandari, Phys. Rev. Lett. **60**, 2339 (1988).

[32] Y.-S. Wu and H.-Z. Li, Phys. Rev. B **38**, 11907 (1988).

[33] Y.-Q. Ma and S. Chen, Phys. Rev. A **79**, 022116 (2009).

[34] M. Kolodrubetz, V. Gritsev, and A. Polkovnikov, Phys. Rev. B **88**, 064304 (2013).

[35] J. B. Hartle and S. W. Hawking, Phys. Rev. D **28**, 2960 (1983).

[36] A. Silva, Phys. Rev. Lett. **101**, 120603 (2008).

[37] S. Sachdev, *Quantum Phase Transitions* (Cambridge University Press, Cambridge, UK, 2011).

[38] A. C. M. Carollo and J. K. Pachos, Phys. Rev. Lett. **95**, 157203 (2005).

[39] S.-L. Zhu, Phys. Rev. Lett. **96**, 077206 (2006).

[40] A. Hamma, arXiv:quant-ph/0602091.

[41] J. Provost and G. Vallee, Comm. Math. Phys. **76**, 289 (1980).

[42] D. J. Thouless, J. Math. Phys. **35**, 5362 (1994); T. Frankel, *The Geometry of Physics: An Introduction* (Cambridge University Press, Cambridge, UK, 2004).

[43] M. P. L. Heyl, *Nonequilibrium Phenomena in Many-Body Quantum Systems* (Ludwig-Maximilians-Universität München, Munich, Germany, 2012).

[44] R. Resta, J. Phys.: Condens. Matter **12**, R107 (2000).

[45] M. B. Plenio and P. L. Knight, Rev. Mod. Phys. **70**, 101 (1998).